AGU PUBLICATIONS

Geochemistry, Geophysics, Geosystems

TECHNICAL BRIEF

10.1002/2014GC005309

REDBACK: Open-source software for efficient noise-reduction in plate kinematic reconstructions

G. Iaffaldano[1], R. Hawkins[1], T. Bodin[2], and M. Sambridge[1]

[1]Research School of Earth Sciences, Australian National University, Canberra, ACT, Australia, [2]Department of Earth and Planetary Sciences, University of California at Berkeley, Berkeley, California, USA

Key Points:

- Finite-rotation noise hampers plate kinematic reconstructions
- Bayesian Inference is effective in reducing noise impact
- REDBACK implements Bayesian Inference for plate kinematic reconstructions

Correspondence to:
G. Iaffaldano,
giampiero.iaffaldano@anu.edu.au

Citation:
Iaffaldano, G., R. Hawkins, T. Bodin, and M. Sambridge (2014), REDBACK: Open-source software for efficient noise-reduction in plate kinematic reconstructions, *Geochem. Geophys. Geosyst.*, *15*, 1663–1670, doi:10.1002/2014GC005309.

Received 20 FEB 2014
Accepted 9 APR 2014
Accepted article online 15 APR 2014
Published online 30 APR 2014

Abstract Knowledge of past plate motions derived from ocean-floor finite rotations is an important asset of the Earth Sciences, because it allows linking a variety of shallow-rooted and deep-rooted geological processes. Efforts have recently been taken toward inferring finite rotations at the unprecedented temporal resolution of 1 Myr or less, and more data are anticipated in the near future. These reconstructions, like any data set, feature a degree of noise that compromises significantly our ability to make geodynamical inferences. Bayesian Inference has been recently shown to be effective in reducing the impact of noise on plate kinematics inferred from high-temporal-resolution finite-rotation data sets. We describe REDBACK, an open-source software that implements transdimensional hierarchical Bayesian Inference for efficient noise-reduction in plate kinematic reconstructions. Algorithm details are described and illustrated by means of a synthetic test.

1. Introduction

REDBACK is a software for efficient reduction of noise in plate kinematic reconstructions. It has been developed by the authors at the Research School of Earth Sciences of the Australian National University, as part of the AuScope-AGOS Inversion Laboratory. REDBACK is released open source under the GNU General Public License (GPL), and can be obtained by logging onto http://www.iearth.org.au/codes/REDBACK or by contacting the corresponding author. REDBACK is deliberately designed to perform efficiently on personal computers, and is available for Unix and Windows platforms/operating systems. Its strengths are easiness of use and computational efficiency. Users include scientists and industry researchers studying plate motions and their changes through geological time.

The theory of plate tectonics [e.g., *Wilson*, 1965; *McKenzie and Parker*, 1967; *Morgan*, 1968; *Le Pichon*, 1968] is widely recognized as the unifying paradigm that underpinned scientific progress over the past four decades in virtually all areas of the Earth Sciences. Central to the plate tectonic theory are reconstructions of past global plate motions [e.g., *Gordon and Jurdy*, 1986; *Stampfli and Borel*, 2002; *Torsvik et al.*, 2010]. These are crucial to interpret the geological record of Earth, and more specifically to derive important inferences on plate dynamics [e.g., *Iaffaldano and Bunge*, 2009; *Copley et al.*, 2010], mantle convection [e.g., *Ricard et al.*, 1993; *Bunge et al.*, 1998], dynamic topography [e.g., *Moucha et al.*, 2008], and sea-level change [e.g., *Braun*, 2010, and references therein], among others. Tectonic plate motions and their temporal changes are well described, under the approximation of lithosphere rigidity [e.g., *Gordon*, 1998], by stage Euler vectors (i.e., time-dependent vectors oriented as the axes of instantaneous rotation and whose magnitudes are equal to instantaneous angular velocities). Stage Euler vectors are readily obtained by differentiating, according to the algebra of rotation matrices, finite rotations of Earth's lithosphere, which express the relative paleoposition of two adjacent plates at some time in the geological past. One infers finite rotations from observations of the ocean-floor structure (i.e., fracture zones) as well as of the imprint that the past Earth's magnetic field left on it (i.e., magnetic lineations) [e.g., *Chang*, 1988; *Royer and Chang*, 1991]. After four decades of geophysical exploration, the fraction of present-day ocean floor mapped allows the scientific community to infer global plate motions for the past ~170 Myr at a temporal resolution of ~10 Myr [e.g., *Müller et al.*, 2008; *Torsvik et al.*, 2010]. While these progresses from plate kinematicists are encouraging, geodynamicists wish for finer temporal resolution of reconstructions, in order to better constrain their models. Today, significant and important efforts are being made toward mapping the magnetization/structure of some portions of the ocean floor (e.g., Carlsberg Ridge, Southeast Indian Ridge) at even finer resolution than what is already available. The result is that we are beginning to infer relative plate-motion changes over the past ~20 Myr—in some cases even ~40 Myr—at the unprecedented temporal resolution of 1 Myr or less [*Croon et al*., 2008; *Merkouriev and DeMets*, 2008; *Bull et al*., 2010; *Fournier et al*., 2010]. These advances are indeed promising in terms of achieving finer global coverage, and more high-temporal-resolution reconstructions are anticipated for the near future.

2. Noise in Finite-Rotation Data Sets

Finite-rotation data sets, like any data set, feature noise. This may be substantial, and consequently hamper our ability to build on kinematic reconstructions and derive geophysical inferences. In the specific case, finite-rotation noise does not relate to the accuracy of instrumentation and facilities used in mapping the magnetization/structure of the ocean floor (e.g., accuracy of navigation positioning in ship surveys). Instead, it arises from the challenge of identifying clearly magnetic lineations of the ocean floor [e.g., *Dyment and Arkani-Hamed*, 1995], often from insufficiently long segments of slowly spreading ridges [*Patriat et al*., 2008]. In fact, raw data of ocean-floor magnetization, despite their accuracy, necessarily require choices to be made about where to chart the imprint of paleoinversions of Earth's magnetic field. Such choices are inevitably subjective and thus give rise to noise in the inferred magnitude of past plate-motion changes. In addition, errors may also arise from the calibration accuracy of geomagnetic reversal time scales [e.g., *Heirtzler et al*., 1968; *Cande and Kent*, 1995], which impacts on the magnitude as well as timing of past kinematic changes—although more precise astronomical calibration [e.g., *Shackleton et al*., 1990] helps reducing this bias for the past ~25 Myr. Finally, inferring past rotation poles of adjacent plates from observations of ocean-floor fracture zones may be prone to even greater biases. Ideally, one should collect a statistically significant number of repeated measurements of the ocean-floor magnetization/structure in order to minimize the impact of noise. In practice, this becomes unfeasible because of the costs associated with marine and airborne surveys.

The issue of noise in plate finite rotations has been recognized since the very first kinematic reconstructions [e.g., *Hellinger*, 1981]. We report below a simple example used by *Iaffaldano et al*. [2013] to illustrate that, as the temporal resolution of finite-rotation reconstructions increases, noise impacts progressively more on the inferred Euler vectors. Let θ_1 and $\theta_2 > \theta_1$ be two finite rotations, derived from the ocean-floor magnetization, that constrain the relative paleoposition of two spreading plates at times t_1 and t_2. The axis about which plates rotate, as well as the spreading center separating them, are both assumed to remain fixed from t_1 to t_2. Such a simplification allows scalar algebra, rather than the algebra of rotation matrices; but the main inferences from this example hold true also for 3-D rotations about non-fixed axes. The two plates accrue an angle equal to $(\theta_2 - \theta_1)$ during the interval of time between t_1 and t_2. Therefore, $(t_2 - t_1)$ is a measure of the temporal resolution of the reconstruction. Let $\Delta\theta$ be the amount of noise present in both θ_1 and θ_2—that is, the random departure from the true angles. Because of the origin of finite-rotation noise, $\Delta\theta$ does not depend on the particular resolution of the reconstruction. The *reconstructed* angular velocity of the Euler vector describing the relative motion from t_1 to t_2 is thus $\omega_r = (\theta_2 - \theta_1)/(t_2 - t_1)$. However, the presence of noise implies that the *true* angular velocity is in fact anywhere in range $\omega_t = (\theta_2 - \theta_1)/(t_2 - t_1) \pm 2\Delta\theta/(t_2 - t_1)$. The last term in ω_t represents the departure of the *reconstructed* angular velocity from the *true* one, and arises from the presence of noise $\Delta\theta$. It is then evident that at finer temporal resolution of reconstructions, the denominator $(t_2 - t_1)$ becomes smaller, and consequently the error term becomes progressively larger. Since previous reconstructions featured a relatively low temporal resolution of ~10 Myr or more [e.g., *Gordon and Jurdy*, 1986; *Stampfli and Borel*, 2002; *Torsvik et al*., 2010], the issue of noise has been classically deemed of second-order importance, because a likely small noise-to-signal ratio was propagated to the associated plate motions. However, with the modern levels of temporal resolution (~1 Myr) [e.g., *Croon et al*., 2008; *Merkouriev and DeMets*, 2008; *Bull et al*., 2010; *Fournier et al*., 2010], the impact of noise on the inferred kinematic histories increases to the point that reconstructions become geodynamically implausible, in the sense that geological process may hardly build torque upon plates at the rate necessary to explain the reconstructed kinematics. This was discussed in detail by *Iaffaldano et al*. [2012, 2013].

Since the temporal resolution of reconstructions amplifies the impact of noise, it has become standard practice to average through time—also referred to as smoothing—finite-rotation series, in the hope of mitigating such a bias. The limited efficiency of smoothing in retrieving actual plate-motion changes can be addressed by means of a simple 1-D synthetic test. We imagine that the angular velocity of a plate varies every 1 Myr or so, according to an imposed pattern (Figure 1, blue). We choose plate-like values on the

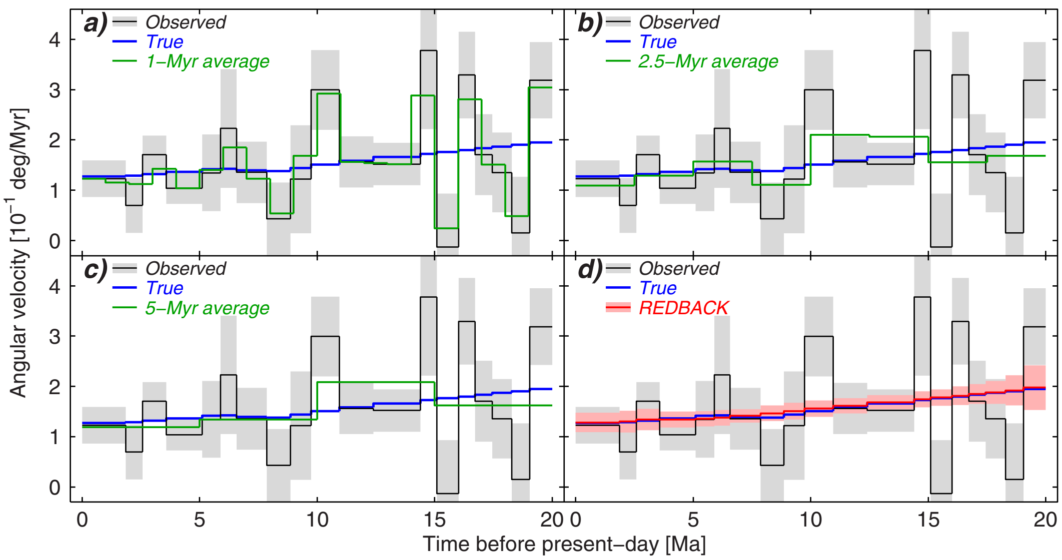

Figure 1. Synthetic test showing an Earth-like plate-motion pattern (in blue, deemed as true), as well as the same pattern, upon addition of Gaussian noise and uncertainties (in black, deemed as observed—see text for details). (a) Result of smoothing the observed kinematic pattern by averaging every 1 Myr (in green). (b and c) Same as Figure 1a, but using an averaging window of 2.5 and 5 Myr, respectively. (d) Result of applying REDBACK to the observed kinematic pattern. The solution of REDBACK (in red) (i) retrieves well the true kinematic patters, (ii) comes at no loss of temporal resolution with respect to the original data, and (iii) features small uncertainty (red-shaded areas—see text for details).

order of 10^{-1}deg/Myr [e.g., *DeMets et al*., 2010; *Argus et al*., 2011], and a pattern of temporal variations mimicking a slow-down by some 40% in 20 Myr—in line with evidence from previous kinematic reconstructions [e.g., *Torsvik et al*., 2010]. We deem this as the true angular velocity. We then add random Gaussian noise to it, to obtain a pattern that departs substantially from the true one, and thus could represent the result of differentiating observed noisy finite rotations (Figure 1, black). Specifically, for each temporal stage over the modeled past 20 Myr, the value of noise is drawn from a Gaussian distribution with standard deviation on the order of half of the variability of actual, high-temporal resolution Euler vectors that have been recently published [e.g., *Merkouriev and DeMets*, 2006, 2008]. In other words, we cast a realistic level of noise into the true pattern. Finally, we add real uncertainties taken from the covariances of the Capricorn/Somalia motion since ~20 Ma of *Bull et al*. [2010] (Figure 1, gray-shaded area around black lines). Such a choice is arbitrary, and we could have equally taken uncertainties from the India/Somalia reconstruction of the same authors, or from the Eurasia/North America data set of *Merkouriev and DeMets* [2008]. We deem this pattern as noisy observations. Green lines in Figures 1a–1c show the result of averaging the observed angular velocity every 1, 2.5, and 5 Myr, respectively. From the comparison of true and inferred kinematics, several drawbacks associated with averaging, and more generally with smoothing, are evident: (i) It systematically downgrades the native temporal resolution of observed finite rotations that are derived from hard-won measurements. (ii) It does not yield a unique solution, because of the dependence on the chosen time window. (iii) Any such choice remains arbitrary, and leads to a pattern that has little resemblance with the true one. While we use a 1-D example, these issues apply also to realistic 3-D cases. In a notable paper, *Merkouriev and DeMets* [2006] resorted to more elegant and sophisticated methods such as bootstrapping; nonetheless these issues persist. With this example we do not question, or dismiss the usefulness of finite-rotation data sets. In fact, we maintain that these are invaluable to Earth scientists to reconstruct the paleogeography of tectonic plates, and indeed welcome the recent advances [e.g., *Croon et al*., 2008; *Merkouriev and DeMets*, 2008; *Bull et al*., 2010; *Fournier et al*., 2010]. Instead, our goal with REDBACK is to bridge an objective technical gap in our ability to unravel true plate-motion histories from reconstructed finite rotations.

3. REDBACK

The theory underlying REDBACK is the well-known Bayesian Inference [e.g., *Bayes*, 1763], implemented in the recently developed transdimensional hierarchical fashion [e.g., *Malinverno and Briggs*, 2004; *Sambridge* *et al*., 2006]. This probabilistic approach to data inference has already been discussed and applied to several problems in the Earth Sciences [e.g., *Malinverno*, 2002; *Bodin and Sambridge*, 2009; *Gallagher*, 2012; *Tkalcić et al*., 2013]. *Iaffaldano et al*. [2012, 2013, 2014] used it for the first time in the context of tectonic plate finite rotations, to reduce the impact of noise in a number of recently published plate-motion histories (i.e., India/Somalia, Eurasia/North America, Pacific/Antarctica, India/Eurasia, and Nubia/Somalia). Generally speaking, transdimensional hierarchical Bayesian Inference allows one to recognize, in a noisy time series of observations, the level of data noise, and thus the level of complexity of the true series. In the case of finite-rotation time series, this effectively means being able to distinguish temporal kinematic changes that are likely to be real changes in plate motion due to geological processes, from the artifacts originating from noise in finite rotations. Bayesian Inference is therefore well suited to identifying plate-motion changes from noisy records.

REDBACK implements transdimensional hierarchical Bayesian Inference through the following algorithm: initially, a 3-D model **m** that may represent the true series of finite-rotation angle and pole through geological time is randomly generated. Such a 3-D model consists of three 1-D time series that, together, parameterize finite rotations: one series for the longitude of the rotation pole, one for the latitude, and one for the rotated angle between adjacent tectonic plates. One does not need to have any particular a priori knowledge as to the exact number, magnitude, or timing of true changes, because these are treated as free parameters. Further, such a model is initially considered just as likely to be a faithful realization of the truth as any other randomly generated model. In the jargon of Bayesian Inference, this corresponds to choosing a uniform prior probability density distribution—or simply prior—within reasonable bounds. In simpler words, it means initially assigning to **m** a probability p of being the faithful realization of the truth before even looking at the data **d**. The prior is typically indicated with $p(\mathbf{m})$. REDBACK assumes that $p(\mathbf{m})$ is uniform within bounds set ad hoc for the particular data set at hand. Specifically, for each time series of the 3-D finite-rotation data set (longitude of the rotation pole, latitude of the same and rotated angle), the prior is set to a constant uniform value in the interval from little less than the minimum to little more than the maximum of the time series. Instead, outside such an interval the prior is set to zero. Thus, values within the minimum and the maximum of the data time series are initially considered to be equally probable; while values smaller than the data minimum or larger than the data maximum are not considered at all. Such a choice is logical for the time series of rotated angle, which is by definition monotonically increasing from younger to older time stages. We regard such a prior to be a reasonable choice also for the time series of rotation-axis longitude and latitude. In fact, in noisy finite-rotation data sets the geographical region over which longitude and latitude scatter is typically so wide [e.g., *Iaffaldano et al*., 2012, 2013] that the true values will very likely fall in it. Next, REDBACK estimates how well the model **m** fits (i.e., explains) the observed finite rotations. In the jargon of Bayesian Inference, this means estimating the *likelihood* of observing the input data set **d**, given the model time series at hand **m**. The likelihood is indicated with $p(\mathbf{d}|\mathbf{m})$ (generally, the expression $a|b$ means a given, or conditional on, b), and is defined as follows:

$$p(\mathbf{d}|\mathbf{m})=\frac{1}{2\pi\sqrt{|C|}}\exp\left[-\frac{1}{2}(\mathbf{d}-\mathbf{m})^{T}C^{-1}(\mathbf{d}-\mathbf{m})\right] \quad (1)$$

where C is the covariance of data and T indicates the transpose of the difference vector $(\mathbf{d}-\mathbf{m})$ between data and model. Because of the negative sign within the exponential, the smaller such a distance is, the greater the likelihood of **d**, given **m**, will be.

REDBACK uses this level of fit to estimate the probability that finite-rotation model **m** is in fact a faithful realization of the truth, given the data **d**. Such a probability estimate is referred to as the *posterior* $p(\mathbf{m}|\mathbf{d})$, because it is determined after comparing models to observations. In Bayesian Inference, the posterior is proportional to the likelihood times the prior, that is, $p(\mathbf{m}|\mathbf{d}) \propto p(\mathbf{d}|\mathbf{m})\times p(\mathbf{m})$. Sampling the posterior across the space of possible models is the core of Bayesian Inference. Since REDBACK employs a uniform prior within bounds derived from the input data, the posterior distribution of probability is in fact shaped as the likelihood distribution across the model space. Sampling of the entire space of models can be computationally expensive (sometimes prohibitively so), especially if the model space stretches across dimensions. To sample the posterior in a computationally efficient fashion, REDBACK implements a Monte Carlo Markov Chain [see *Sisson*, 2005, for a review] that, instead of systematically sampling the entire model space,

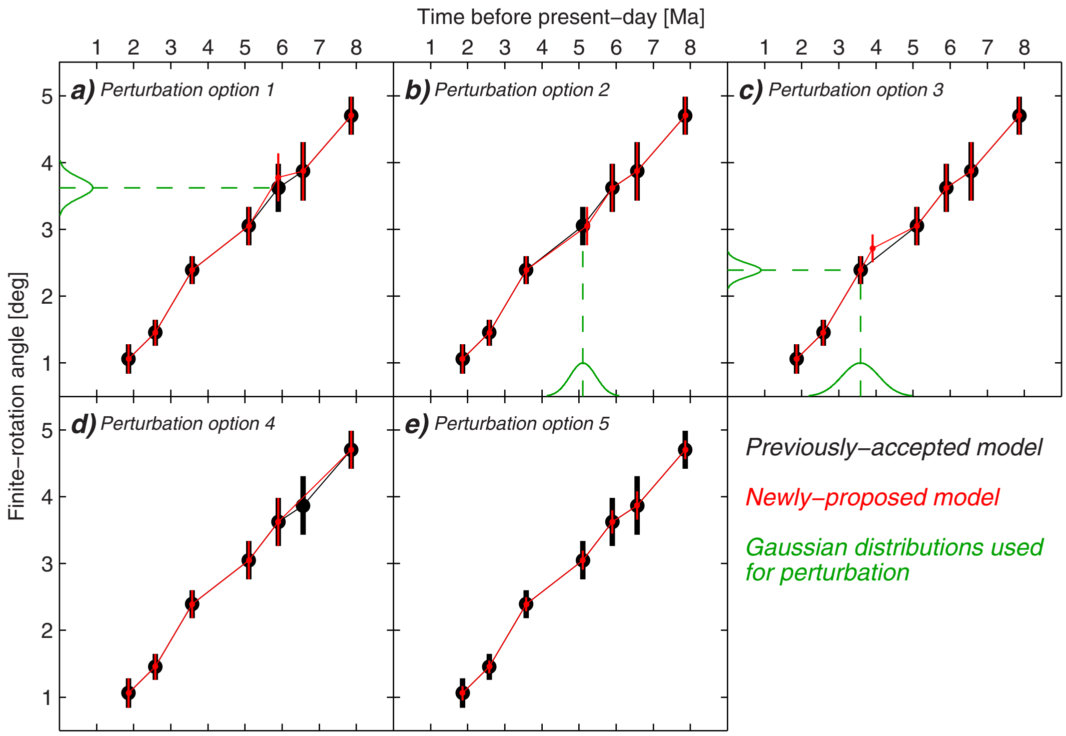

Figure 2. Examples of options that REDBACK uses to perturb a previously accepted model (in black) into a newly proposed one (in red) within the Monte Carlo Markov Chain. For simplicity, examples are shown for an imaginary 1-D time series of finite-rotation angles (dots) and associated uncertainties (vertical bars) since ~8 Ma. In fact, REDBACK uses these options to propose a new 3-D model consisting of three time series: longitude, latitude, and rotated angle of finite rotations. Gaussian distributions used to draw the perturbation values are in green. Figures 2a–2e show, respectively, options 1–5 described in the main text. For the latter example, uncertainties on the proposed model have been reduced. However, they could also be increased, depending on the parameters set by the user. All input parameters are described in more detail in the user manual associated with REDBACK.

samples a subspace in which models are ultimately distributed like the posterior. Specifically, after having estimated the likelihood of model **m** through equation (1), REDBACK perturbs **m** to generate a new model $\mathbf{m}'$. It then (i) compares $\mathbf{m}'$ to data as well to **m**, and—on the basis of such a comparison—(ii) accepts or rejects it as a faithful realization of the truth. In case of rejection, a new model is randomly generated. Instead, in case of acceptance, the Markov Chain moves to a further model generated by perturbing the previously accepted one $\mathbf{m}'$. Acceptance criteria take into account the likelihood of previous and subsequent models, and in general depend on the type of perturbation used by REDBACK. They are described in the following.

In moving the Markov Chain from one accepted model to the next proposed one, REDBACK randomly selects a type of perturbation—or move—among the following five options: (1) one single plate-motion change cast within the previously accepted model of finite rotations is perturbed. Effectively, this is readily achieved by perturbing one single finite rotation of the model series. Its new value is drawn from a Gaussian distribution that is centered about the previous value, and features a standard deviation chosen by the user. In Figure 2a, we show a schematic example of how this option would perturb an imaginary time series of rotated angles. REDBACK then computes the probability α that $\mathbf{m}'$ is a better realization of the truth than **m**. Specifically, $\alpha = \min\left[1, p(\mathbf{d}|\mathbf{m}')/p(\mathbf{d}|\mathbf{m})\right]$. If α is greater than a threshold drawn each time from a uniform random distribution between 0 and 1, then $\mathbf{m}'$ is accepted into the Markov Chain. Otherwise it is rejected, and a new model is generated by perturbing **m**. In other words, if the likelihood of $\mathbf{m}'$ is greater than that of **m**, then $\mathbf{m}'$ will certainly be accepted. Otherwise, $\mathbf{m}'$ might still be accepted depending on the always-new value of the acceptance threshold. Changing such a threshold for every proposed move ensures, over a large number of proposals, that no particular standards for acceptance are enforced. (2) The timing of one plate-motion change cast within the previously accepted model of finite-rotation series is perturbed. To this end, the time associated to one randomly selected finite rotation of the model is moved by an amount drawn from a Gaussian distribution with standard deviation chosen by the user (see example in Figure 2b). The expression of probability α and acceptance/rejection criterion is the same of option (1). (3) A new plate-motion change is cast into the previously accepted model. This is achieved by adding one finite rotation to the model. The new rotation values (time and magnitude) are drawn from Gaussian distributions centered around a randomly selected, previously accepted one, and featuring standard deviations chosen by the user (see example in Figure 2c). In this case, the probability α that $\mathbf{m}'$ is a better realization of the truth than $\mathbf{m}$ assumes a slightly different expression. Let us indicate with $\Delta\mathbf{m}$, the range of values that REDBACK may possibly assign to proposed models. Let us also indicate with m'_j the new finite rotation added to propose $\mathbf{m}'$, and with m_i the value that the previously accepted model $\mathbf{m}$ would have at the newly-cast time associated with m'_j. Finally, let $N_{m_i,\sigma^2}(m'_j)$ denote the value that the Gaussian distribution—centered around m_i and featuring standard deviation σ used to generate m'_j—assumes at m'_j. Then $\alpha=\min\left[1, 1/\Delta\mathbf{m}\times p(\mathbf{d}|\mathbf{m}')/p(\mathbf{d}|\mathbf{m})\times N^{-1}_{m_i,\sigma^2}(m'_j)\right]$. The acceptance/rejection criterion is the same of option (1). (4) A plate-motion change cast into the previously accepted model is removed. This is achieved by randomly selecting and discarding one finite rotation from the previously accepted model (Figure 2d). Let us indicate with m_i the finite rotation removed from $\mathbf{m}$ to propose $\mathbf{m}'$, and with m'_j the value that $\mathbf{m}'$ assumes at the time associated with m_i. Since option (4) may be considered the reverse of (3), in this case $\alpha=\min\left[1, \Delta\mathbf{m}\times p(\mathbf{d}|\mathbf{m}')/p(\mathbf{d}|\mathbf{m})\times N_{m_i,\sigma^2}(m'_j)\right]$, while the acceptance/rejection criterion is the same of option (1). Options (3) and (4) implement the transdimensional character of the inference algorithm. (5) Covariances associated with the observed, noisy finite rotations, which provide the associated uncertainty, are scaled by a factor, also referred to as *hierarchical parameter*. The value of the hierarchical parameter may be smaller than 1—expressing the user's hypothesis that nominal uncertainty on data might have been overestimated—or greater than 1—expressing, instead, the hypothesis of underestimation. Such a value is drawn from a Gaussian distribution centered around the previously accepted hierarchical-parameter value (or randomly selected in the first instance), and featuring standard deviation chosen by the user (see example in Figure 2e). The expression of probability α and acceptance/rejection criterion are the same of option (1). Option 5 impacts on the computed level of data fit (i.e., on the distance between subsequent models and data), and therefore on sampling of the posterior. All the probability formula and acceptance criteria follow the well-known criterion of Metropolis-Hasting [*Metropolis et al.*, 1953; *Hasting*, 1970], which ensures that a better-fitting model with respect to the previously accepted one (i.e., $\alpha = 1$) will always be accepted, while a poorer model (i.e., $\alpha < 1$) will be accepted with some probability. This avoids, for instance, the fact that the Markov Chain systematically rejects all proposed models once a local maximum of the likelihood distribution has been sampled.

REDBACK iterates such a procedure a number of times set by the user, with recommended values being on the order of million. We note that the Monte Carlo Markov Chain character of the procedure only ensures computational efficiency in sampling—particularly on personal computers, for which REDBACK is intended. However, the effectiveness of the sampling (i.e., whether the ensemble of accepted models do ultimately distribute like the posterior probability density) relies predominantly on choices made by the user, and more specifically on the standard deviations used in the Markov Chain algorithm for perturbing the previously accepted model into the next one. It is straightforward to imagine that if the user chooses values for these standard deviations which are too small, then the perturbed model is likely to be very similar to the previously accepted one. As a consequence, the iteration will effectively dwell on a particular subregion of the model space to sample. In fact, since small standard-deviation values enforce resemblance between two consecutively accepted models, it is unlikely, during the iteration process, to move away from such a subregion. Instead, if the user selects standard-deviation values which are too large, then the iteration will quickly move from one subregion of the model space to a different one, likely without having sampled it enough to obtain sufficient resemblance to the posterior. For a more technical and comprehensive review of these notions, see *Gallagher et al.* [2009]. User's choices impact on the rate at which the posterior is sampled throughout the model space, and hence on the efficiency of the algorithm. However, all choices will, eventually, lead to unbiased sampling of the posterior. While this is true in theory, in practice the user needs to make sure that reasonable, if not optimal, sampling is achieved within the preset number of iterations. Typically, first-order indications that this has been achieved are the smoothness and shape of histograms for the distribution of input parameters across the ensemble of accepted models. In the user manual associated with REDBACK, we provide more detailed examples of how to follow such a criterion. In this sense, user's choices are crucial to the effectiveness of REDBACK in retrieving true plate-motion changes from noisy finite-rotation data sets.

The final solution REDBACK provides is not a single best-fitting model among the ensemble that has been sampled, nor the most probable one based on the posterior. It is, rather, the mean of the whole ensemble of accepted models. In addition, REDBACK computes covariances around the mean from the entire ensemble. This provides the user with a confidence interval for the solution found by REDBACK. In a way, the algorithm that REDBACK implements is not too dissimilar to what experimentalists do in the laboratory when taking repeated measurements of a given observable. In estimating the most representative value of an observable, one typically repeats the same measurement for a statistically significant number of times. The most representative value of the observable is not any particular one of these measurements, nor the most certain one. Rather, it is the weighted mean, which takes into account the uncertainty of each single measurement, but weighs more the most certain ones. Instead of repeated measurements and associated uncertainties, REDBACK deals with an ensemble of millions of models, and computes the final solution as the mean of such an ensemble. The fact that the accepted models are distributed in a way similar to the posterior implies that their mean effectively corresponds to the weighted mean of all possible models—where weights are determined by the posterior distribution of probability. Finally, at first glance one may think that models featuring a greater number of plate-motion changes may seem prone to fit the noisy finite rotations better, thus yielding higher posterior probability with respect to simpler models. However, it is well established that transdimensional hierarchical Bayesian Inference follows the principle of *natural parsimony* [*MacKey*, 2003], where preference always falls on the least complex explanation of observations.

In Figure 1d, we show the solution provided by REDBACK for the simple 1-D synthetic test described above. The red line is the weighted mean of the ensemble, while the red-shaded area around it represents the confidence the user should have in such a solution, expressed in the form of covariances similar to those typically associated with finite-rotation or Euler-vector data sets. At each time stage, REDBACK computes the matrix C_{ij} for the covariance of the ensemble using the standard formula $C_{ij}=E[m_i \cdot m_j]-E[m_i] \cdot E[m_j]$—where $i, j=1, 2, 3$ indicate the axes—$\hat{x}, \hat{y}$, and $\hat{z}$—of the orthonormal reference frame, m indicates the model component along a particular axis and $E[...]$ is the expected value—or mean—of the argument within brackets. Comparing Figures 1a–1c with Figure 1d clearly indicates the advantages associated with REDBACK: (i) it offers a superior capability to retrieve the true pattern of kinematic changes, compared to more classical smoothing methods. (ii) Covariances on the stage Euler vectors in output remain small. (iii) The solution comes at no loss of temporal resolution with respect to the original finite-rotation data set. Outputs of REDBACK include noise-reduced Euler vectors and associated finite rotations (both completed with covariances), as well as few useful auxiliary files that serve for diagnostics. Importantly, we built into REDBACK the option of sampling the solution at different temporal stages than the native ones. This is particularly suited for combining different finite-rotation data sets in reconstructing, for instance, the relative convergence between subducting and overriding plates. To our knowledge, no other algorithm is capable of achieving this level of accuracy in estimation of true plate motions.

4. Conclusions

REDBACK has been developed for efficient noise reduction in plate kinematic reconstructions. We explained the origin of noise in finite rotations, and illustrated the impact it has on the inference of plate kinematics. We outlined the algorithm implemented within REDBACK, which builds on the increasingly popular approach known as transdimensional hierarchical Bayesian Inference. By resorting to a synthetic test, we showed that REDBACK offers a superior ability to retrieve true plate-motion changes from noisy finite-rotation data sets, as opposed to more classical smoothing methods. REDBACK is released open source under the GNU General Public License (GPL), and can be obtained by contacting the corresponding author or by logging onto http://www.iearth.org.au/codes/REDBACK. Users include plate kinematicists, geodynamicists, and anyone making use of tectonic plate motions and their changes through geological time. REDBACK comes with a user manual that includes examples based on synthetic as well as real finite-rotation data sets.

Acknowledgments
G.I. acknowledges support from the Ringwood Fellowship at the Research School of Earth Sciences (RSES) of the Australian National University. Authors acknowledge support from the AuScope-AGOS Inversion Laboratory. AuScope Ltd. is funded under the National Collaborative Research Infrastructure Strategy (NCRIS) and the Education Investment Fund (EIF), both Australian Commonwealth Government Programs. Authors thank two anonymous reviewers as well as the Editor, Thorsten Becker, for their careful and constructive comments. Authors are grateful to M. Salmon for support.

References

Argus, D. F., R. G. Gordon, and C. DeMets (2011), Geologically current motion of 56 plates relative to the no-net-rotation reference frame, *Geochem. Geophys. Geosyst.*, *12*, Q11001, doi:10.1029/2011GC003751.
Bayes, T. (1763), *An Essay Towards Solving A Problem in the Doctrine of Chances*, R. Soc. of London, London.
Bodin, T., and M. Sambridge (2009), Seismic tomography with the reversible jump algorithm, *Geophys. J. Int.*, *178*, 1411–1436.

Braun, J. (2010), The many surface expressions of mantle dynamics, *Nat. Geosci.*, *3*, 825–833.
Bull, J. M., C. DeMets, K. S. Krishna, D. J. Sanderson, and S. Merkouriev (2010), Reconciling plate kinematic and seismic estimates of lithospheric convergence in the central Indian Ocean, *Geology*, *38*, 307–310.
Bunge, H.-P., M. A. Richards, C. Lithgow-Bertelloni, J. R. Baumgardner, S. P. Grand, and B. A. Romanowicz (1998), Time scales and heterogeneous structure in geodynamic earth models, *Science*, *280*, 91–95.
Cande, S. C., and D. V. Kent (1995), Revised calibration of the geomagnetic polarity timescale for Late Cretaceous and Cenozoic, *J. Geophys. Res.*, *100*, 6093–6095.
Chang, T. (1988), Estimating the relative rotation of two tectonic plates from boundary crossings, *J. Am. Stat. Assoc.*, *83*, 1178–1183.
Copley, A., J.-P. Avouac, and J.-Y. Royer (2010), India-Asia collision and the Cenozoic slowdown of the Indian plate: Implications for the forces driving plate motions, *J. Geophys. Res.*, *115*, B03410, doi:10.1029/2009JB006634.
Croon, M. B., S. C. Cande, and J. M. Stock (2008), Revised Pacific-Antarctic plate motions and geophysics of the Menard Fracture Zone, *Geochem. Geophys. Geosyst.*, *9*, Q07001, doi:10.1029/2008GC002019.
DeMets, C., R. G. Gordon, and D. F. Argus (2010), Geologically current plate motions, *Geophys. J. Int.*, *181*, 1–80.
Dyment, J., and J. Arkani-Hamed (1995), Spreading-rate-dependent magnetization of the oceanic lithosphere inferred from the anomalous skewness of marine magnetic anomalies, *Geophys. J. Int.*, *121*, 789–804.
Fournier, M., et al. (2010), Arabia-Somalia plate kinematics, evolution of the Aden-Owen-Carlsberg triple junction, and opening of the Gulf of Aden, *J. Geophys. Res.*, *115*, B04102, doi:10.1029/2008JB006257.
Gallagher, K. (2012), Transdimensional inverse thermal history modeling for quantitative thermochronology, *J. Geophys. Res.*, *117*, B02408, doi:10.1029/2011JB008825.
Gallagher, K., K. Charvin, S. Nielsen, M. Sambridge, and J. Stephenson (2009), Markov chain Monte Carlo (MCMC) sampling methods to determine optimal models, model resolution and model choice for earth science problems, *Mar. Pet. Geol.*, *26*, 525–535.
Gordon, R. G. (1998), The plate tectonic approximation: Plate nonrigidity, diffuse plate boundaries, and global plate reconstructions, *Ann. Rev. Earth Planet. Sci.*, *26*, 615–642.
Gordon, R. G., and D. M. Jurdy (1986), Cenozoic global plate motions, *J. Geophys. Res.*, *91*, 12,389–12,406.
Hasting, W. K. (1970), Monte-Carlo sampling methods using Markov chains and their applications, *Biometrika*, *57*, 97–109.
Heirtzler, J. R., G. O. Dickson, E. M. Herron, W. C. Pitman III, and X. L. Pichon (1968), Marine magnetic anomalies, geomagnetic field reversals, and motions of the ocean floor and continents, *J. Geophys. Res.*, *73*, 2119–2136.
Hellinger, S. J. (1981), The uncertainties of finite rotations in plate tectonics, *J. Geophys. Res.*, *86*, 9312–9318.
Iaffaldano, G., and H.-P. Bunge (2009), Relating rapid plate-motion variations to plate-boundary forces in global coupled models of the mantle/lithosphere system: Effects of topography and friction, *Tectonophysics*, *474*, 393–404.
Iaffaldano, G., T. Bodin, and M. Sambridge (2012), Reconstructing plate-motion changes in the presence of finite-rotations noise, *Nat. Commun.*, *3*, 1048.
Iaffaldano, G., T. Bodin, and M. Sambridge (2013), Slow-downs and speed-ups of India-Eurasia convergence since ~20 ma: Data-noise, uncertainties and dynamic implications, *Earth Planet. Sci. Lett.*, *367*, 146–156.
Iaffaldano, G., R. Hawkins, and M. Sambridge (2014), Bayesian noise-reduction in Arabia/Somalia and Nubia/Arabia finite rotations since ~20 ma: Implications for Nubia/Somalia relative motion, *Geochem. Geophys. Geosyst.*, *15*, doi:10.1002/2013GC005089, in press.
Le Pichon, X. (1968), Sea-floor spreading and continental drift, *J. Geophys. Res.*, *73*, 3661–3697.
MacKey, D. (2003), *Information Theory, Inference, and Learning Algorithms*, Cambridge Univ. Press, New York.
Malinverno, A. (2002), Parsimonious Bayesian Markov chain Monte Carlo inversion in a nonlinear geophysical problem, *Geophys. J. Int.*, *151*, 675–688.
Malinverno, A., and V. A. Briggs (2004), Expanded uncertainty quantification in inverse problems: Hierarchical Bayes and empirical Bayes, *Geophysics*, *69*, 1005–1016.
McKenzie, D. P., and R. L. Parker (1967), The North Pacific: An example of tectonics on a sphere, *Nature*, *216*, 1276–1280.
Merkouriev, S., and C. DeMets (2006), Constraints on Indian plate motion since 20 ma from dense Russian magnetic data: Implications for Indian plate dynamics, *Geochem. Geophys. Geosyst.*, *7*, Q02002, doi:10.1029/2005GC001079.
Merkouriev, S., and C. DeMets (2008), A high-resolution model for Eurasia-North America plate kinematics since 20 ma, *Geophys. J. Int.*, *173*, 1064–1083.
Metropolis, N., A. W. Rosenbluth, M. N. Rosenbluth, A. H. Teller, and E. Telleret (1953), Equation of state calculations by fast computing machines, *J. Chem. Phys.*, *21*, 1087–1092.
Morgan, W. J. (1968), Rises, trenches, great faults, and crustal blocks, *J. Geophys. Res.*, *73*, 1959–1982.
Moucha, R., A. M. Forte, J. X. Mitrovica, D. B. Rowley, S. Quéré, N. A. Simmons, and S. P. Grand (2008), Dynamic topography and long-term sea-level variations: There is no such thing as a stable continental platform, *Earth Planet. Sci. Lett.*, *271*, 101–108.
Müller, R.-D., M. S. C. Gaina, and W.-R. Roest (2008), Age, spreading rates, and spreading asymmetry of the world's ocean crust, *Geochem. Geophys. Geosyst.*, *9*, Q04006, doi:10.1029/2007GC001743.
Patriat, P., H. Sloan, and D. Sauter (2008), From slow to ultraslow: A previously undetected event at the Southwest Indian Ridge at ca. 24 Ma, *Geology*, *36*, 207–210.
Ricard, Y., M. A. Richards, C. Lithgow-Bertelloni, and Y. L. Stunff (1993), A geodynamic model of mantle density heterogeneity, *J. Geophys. Res.*, *98*, 21,895–21,909.
Royer, J.-Y., and T. Chang (1991), Evidence for relative motions between the Indian and Australian plates during the last 20 m.y. from plate tectonic reconstructions: Implications for the deformation of the Indo-Australian plate, *J. Geophys. Res.*, *96*, 11,779–11,802.
Sambridge, M., K. Gallagher, A. Jackson, and P. Rickwood (2006), Trans-dimensional inverse problems, model comparison and the evidence, *Geophys. J. Int.*, *167*, 528–542.
Shackleton, N. J., A. Berger, and W. R. Peltier (1990), An alternative astronomical calibration of the lower Pleistocene timescale based on ODP site 677, *Trans. R. Soc. Edinburgh Earth Sci.*, *81*, 251–261.
Sisson, S. (2005), Transdimensional Markov chains: A decade of progress and future perspectives, *J. Am. Stat. Assoc.*, *100*, 1077–1089.
Stampfli, G. M., and G. D. Borel (2002), A plate tectonic model for the Paleozoic and Mesozoic constrained by dynamic plate boundaries and restored synthetic oceanic isochrons, *Earth Planet. Sci. Lett.*, *196*, 17–33.
Tkalcić, H., M. Young, T. Bodin, S. Ngo, and M. Sambridge (2013), The shuffling rotation of the Earth's inner core revealed by earthquake doublets, *Nat. Geosci.*, *6*, 497–502.
Torsvik, T. H., B. Steinberger, M. Gurnis, and C. Gaina (2010), Plate tectonics and net lithosphere rotation over the past 150 my, *Earth Planet. Sci. Lett.*, *291*, 106–112.
Wilson, J. T. (1965), A new class of faults and their bearing on continental drift, *Nature*, *207*, 343–347.

